Virchows Arch (1998) 433:297–304

ORIGINAL ARTICLE

Horst Zitzelsberger · Ulrike Kulka · Lars Lehmann
Axel Walch · Jan Smida · Michaela Aubele
Thomas Lörch · Heinz Höfler · Manfred Bauchinger
Martin Werner

Genetic heterogeneity in a prostatic carcinoma and associated prostatic intraepithelial neoplasia as demonstrated by combined use of laser-microdissection, degenerate oligonucleotide primed PCR and comparative genomic hybridization

Received: 30 January 1998 / Accepted: 25 May 1998

Abstract We combined laser-assisted microdissection from H&E-stained paraffin sections, degenerated oligonucleotide-primed polymerase chain reaction (DOP-PCR), and comparative genomic hybridization (CGH) to analyse chromosomal imbalances in small tumour areas consisting of 50–100 cells. This approach was used to investigate intratumour genetic heterogeneity in a case of metastatic prostatic adenocarcinoma and chromosomal changes in areas of prostatic intraepithelial neoplasia (PIN) adjacent to the invasive tumour. In four microdissected invasive tumour areas with different histological patterns (acinar, cribriform, papillary and solid) marked intratumour heterogeneity was found by CGH. Recurrent chromosomal imbalances detected in at least two microdissected tumour areas were gains on 1p32→p36, 2p22, 3q21, 7, 8q21→q24, 11q12→q13, 16p12→p13, 17, 19 and loss on 16q23. Additional chromosomal changes were found in only one of the microdissected areas (gains on 16q21→q23, 20q22 and losses on 8p21→p23, 12p11→q12, 12q21→q26, 13q21→q34, 16q12, and 18q22). In PIN, gains on chromosomes 8q21→q24 and 17 were found in both samples investigated (low and high grade PIN), while gains on chromosomes 7, 11q, 12q, 16p, and 20q and losses on 2p, 8p21→p23, 12q were found only in one PIN area. Controls to ensure reliable CGH results consisted in CGH analyses of (i) approximately 80 microdissected normal epithelial cells, which showed no aberrations after DOP-PCR and (ii) larger cell numbers (approximately 10^5 or 10^7 cells) of the primary tumour investigated without DOP-PCR and partially displaying the chromosomal imbalances (gain on 16p12→p13, losses on 2p25, 8p21→p23, 12p11→p12, 12q21→q26, 18q22) found in the small microdissected areas. Microsatellite and FISH analyses further confirmed our CGH results from microdissected cells. The combined approach of laser-assisted microdissection, DOP-PCR and CGH is suitable to identify early genetic changes in PIN and chromosomal imbalances associated with the particular histological patterns of invasive prostatic adenocarcinoma.

Key words Comparative genomic hybridization · Laser-assisted microdissection · DOP-PCR · Prostatic carcinoma · Prostatic intraepithelial neoplasia

H. Zitzelsberger (✉)[1] · L. Lehmann · M. Bauchinger
GSF National Research Center for Environment and Health, Institute of Radiobiology, Neuherberg, Germany

H. Zitzelsberger · J. Smida
Ludwig-Maximilians-Universität München, Institute of Radiation Biology, München, Germany

A. Walch · M. Aubele · H. Höfler
GSF National Research Center for Environment and Health, Institute of Pathology, Neuherberg, Germany

U. Kulka · T. Lörch
IML Instrumenta Wiesloch, Germany

U. Kulka · H. Höfler · M. Werner
Technische Universität München, Institute of Pathology, München, Germany

[1]*Mailing address*:
GSF-Forschungszentrum für Umwelt und Gesundheit, Institut für Strahlenbiologie, Postfach 1129, D-85758 Oberschleißheim, Germany
e-mail: Zitzelsberger@gsf.de
Tel.: +49-(0)89-31873421, Fax: +49-(0)89–31872873

Introduction

Comparative genomic hybridization (CGH) is a fluorescence in situ hybridization (FISH)-based technique that allows the identification of over- and underrepresented DNA sequences throughout the entire genome of tumour samples. Since CGH also permits the analysis of copy number karyotypes from archival paraffin-embedded material [17, 38], retrospective analyses of larger series of tumour samples have become available, providing new potential diagnostic and prognostic cytogenetic markers [4, 15, 31].

In prostate cancer, FISH and CGH analysis has revealed consistent changes on chromosomes 7, 8p, 10, 13q, 16, 17, and 18q [6–9, 16, 20, 26, 27, 30, 34, 41]. However, prostatic carcinoma may exhibit variable histological patterns and also multifocality, contributing to inter- and intratumour heterogeneity [33]. Although a few FISH and microsatellite studies [28, 30] have also suggested intratumour heterogeneity existing at the chromosomal level, the particular changes associated with distinctive histological patterns are largely unknown. Moreover, cytogenetic changes in prostatic intraepithelial neoplasia (PIN), which is often present adjacent to invasive tumours, are poorly characterized [1, 30].

Molecular genetic characterization of morphologically defined cell groups from tissue sections has become feasible through the use of microdissection approaches [3, 12, 35, 43]. Attempts have been made to combine microdissection and CGH analysis, and especially to allow more sensitive detection of chromosomal imbalances by separating tumour areas from stromal cells [23, 38, 42]. Kuukasjärvi et al. [24] concluded from the results of their CGH studies of a dilution series of DNA from a breast cancer cell line that chromosomal imbalances can be reliably detected from as few as two cells. However, the feasibility of CGH analysis on small cell numbers obtained from routinely formalin-fixed specimens has yet to be validated.

In our study, a combined approach with laser-assisted microdissection, degenerated oligonucleotide-primed PCR (DOP-PCR) and CGH was applied for the analysis of intratumour heterogeneity in a prostatic adenocarcinoma. Moreover, this approach was used to study tumour progression, since PIN areas and a lymph node metastasis from the same patient were analysed. The reliability of CGH results was further confirmed by microsatellite analysis and comparative investigation of large cell numbers from frozen or paraffin-embedded tissue and microdissected cell groups (50–100 cells).

Materials and methods

The radical prostatectomy specimen of a 76-year-old man who had not been treated by androgen ablation prior to surgery was obtained immediately after surgery. One portion of the tumour (0.5×0.5×0.5 cm) was frozen in liquid nitrogen. The remaining tissue was fixed in formaldehyde (4%) for 24 h, after which paraffin blocks were prepared according to standard protocols [5]. The diagnosis was established from H&E-stained 5-µm sections, which revealed an acinar adenocarcinoma with a Gleason score of 7 (patterns 2+5). Metastases were present in the lymph nodes dissected from both the left and right fossa obturatoria or vena iliaca. The pTNM classification [36] was pT3a pN2 pMx R1.

For microdissection, a laser microscope system (P.A.L.M., Wolfratshausen, Germany) consisting of a Zeiss Axiovert microscope (Zeiss, Jena, Germany), a pulsed UV-laser (wavelength 337 nm, maximum frequency: 20 pulses/s, pulse duration: 3 ns), and a computer-controlled micromanipulator was used.

Areas containing tumour cells or cells from normal prostatic glands for control were identified on unmounted H&E-stained slides and documented by photography before and after microdissection (Fig. 1). Using a focused UV laser, unwanted cells or tissue areas surrounding the cells of interest were removed. Owing to the extremely high energy density within the focused laser beam (~5 µJ), all biological material was entirely destroyed [13]. Groups of 50–100 cells were subsequently collected from the same slide using the computer-controlled micromanipulator equipped with a sterile gauge needle (Fig. 1). The gauge needle with the attached cells was transferred into a sterile PCR reaction tube containing 20 µl laser buffer (100 mM Tris/HCl, pH 7.5, 100 µg/ml proteinase K). Microdissected specimens were then heated for 3 h at 55°C to allow proteolytic digestion and for 8 min at 100°C to inactivate the proteinase K. Samples were stored at –20°C until use.

DOP-PCR was performed from microdissected tissue (50–100 cells) according to the previously published method [39], with some modification to enhance DNA yields. Topoisomerase I pretreatment [14] was carried out prior to in vitro amplification. Both reactions, topoisomerase I pretreatment and PCR, were performed in a 50-µl reaction volume (3.5 mM $MgCl_2$, 50 mM KCl, 20 mM Tris/HCl, pH 8.4) containing the microdissected and pretreated cells in 20 µl laser buffer, 0.2 mM primer UW4B (5'-CCGACTCGAGNNNNNNATGTGG-3'), and 2 U topoisomerase I (Life Technologies, Eggenstein, Germany). The reaction was incubated for 30 min at 37°C with topoisomerase to relax the template DNA and for 10 min at 90°C to inactivate the enzyme. Subsequently, 4 U Taq polymerase (Perkin Elmer) was added. The PCR reaction consisted of an initial step (10 min at 94°C, one cycle), five cycles with a low annealing temperature (1 min at 94°C, 1.5 min at 30°C, 3 min for transition from 30°C to 72°C, 3 min at 72°C), 35 cycles with a high annealing temperature (1 min at 94°C, 1 min at 62°C, 3 min at 72°C), and a final extension step (10 min at 72°C). The size of DNA fragments and DNA yields of each reaction were checked by agarose gel electrophoresis. DNA yields were additionally determined by fluorimetric measurements.

To avoid contamination of the PCR reactions, the reagents were added in a laminar flow hood using aerosol resistant tips. PCR solutions were additionally checked for possible contamination in PCR reactions, using gene-specific primers for β-actin without template DNA. Control experiments with DNA from IMR-32 cells harbouring known amplifications and deletions were also performed to check the sensitivity and uniformity of DOP-PCR amplification.

As a control of the CGH results from amplified DNA, CGH was performed from a frozen tissue specimen and from paraffin-embedded tissue sections from the same specimen as was used for microdissection of small cell numbers, after scraping the tumour areas using a surgical knife. DNA was extracted according to standard procedures.

Isolated whole genomic tumour DNA, DOP-PCR-amplified tumour samples and normal male reference DNA were labelled with biotin-16-dUTP or digoxigenin-11-dUTP (Boehringer Mannheim, Germany) either by standard nick translation [44] or by a DOP-PCR reaction consisting of 25 cycles (1 min at 94°C, 1 min at 62°C, 3 min at 72°C).

Metaphase preparations for CGH analysis were obtained from peripheral lymphocytes of a healthy male donor according to standard procedures [22]. After hypotonic treatment, fixed cells were dropped onto clean glass slides. Dried slides were aged for 1 week at 37°C and stored in nitrogen gas at –20°C until use.

CGH analysis was performed according to Kallioniemi et al. [21] and du Manoir et al. [10], with modifcations as described elsewhere [25]. Bound, labelled DNA probes were detected by sequential incubations in Cy2-conjugated streptavidin/biotinylated sheep anti-streptavidin (concentration: 10 µg/ml and 5 µg/ml in PNM-buffer consisting of PN buffer plus 5% nonfat dried milk; Dianova Hamburg, Germany) and mouse anti-digoxigenin (concentration: 10 µg/ml PNM; Boehringer Mannheim, Germany)/Cy3-conjugated rat anti-mouse and mouse anti-rat antibodies (each diluted 1:25 in PNM) (Dianova, Hamburg, Germany). After each incubation step, slides were washed twice in PN buffer (0.1 M sodium phosphate pH 8.0, 0.1% nonidet P-40) before the next. To obtain a fluorescence banding pattern, slides were stained with 4',6'-diamidino-2-phenylindole (DAPI) at a concentration of 0.1 µg/ml in antifading solution [19].

CGH images were captured by a black/white video CCD camera using on-chip integration. The three colours were digitized consecutively with specific single colour filter combinations that were changed automatically on a Zeiss Axioplan2 microscope

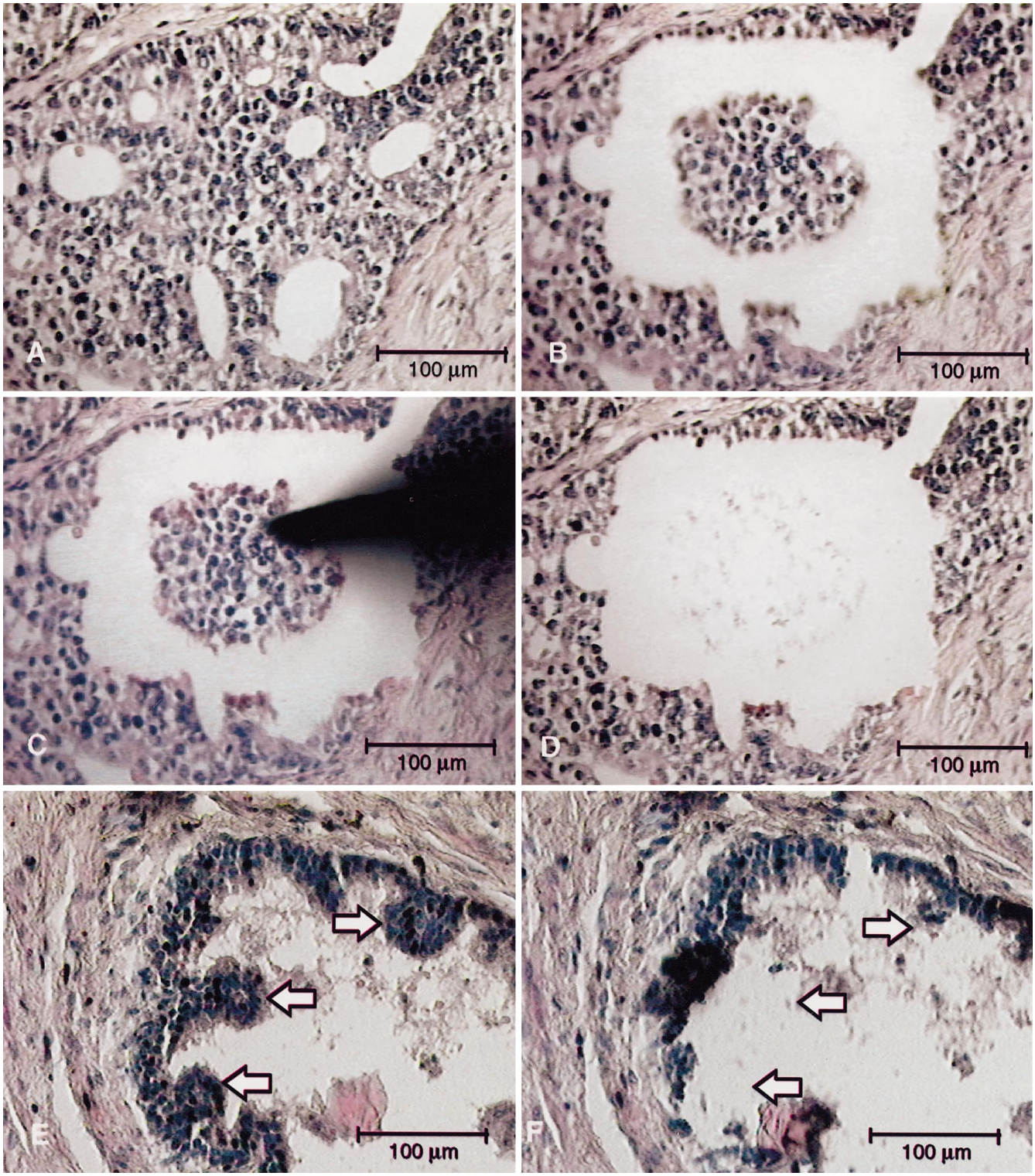

Fig. 1A–F Microdissection from a 5-µm tissue section of a prostatic adenocarcinoma after HE staining: **A** Histological evaluation of the tumour revealed a cribriform pattern. A small tumour area was selected for microdissection. **B** Surrounding tissue ablated by the use of a UV laser. **C** Dissection of a tumour cell group with a computer-assisted micromanipulator equipped with a gauge needle. **D** Tumour area after removal of isolated tumour cells. **E** Histological evaluation of a prostatic intraepithelial neoplasia (PIN) outside the invasive tumour area revealed a low-grade PIN. **F** Dissection of cell groups from the PIN (*arrows*)

(Zeiss, Jena, Germany). For processing of the captured images, image analysis software from MetaSystems (Altlussheim, Germany) was used. For one CGH analysis, at least 10–15 homologues of each chromosome were measured after DAPI karyotyping of 5–10 metaphases. Average ratio profiles were calculated after automatic scaling of the profiles of individual homologous chromosomes of the same length. The average profiles were displayed along with ideograms of the appropriate chromosomes. The standard procedure of interpreting the average red/green ratio profiles is performed by comparing them with fixed ratio thresholds (e.g.,

0.75 and 1.25). If the ratio value is outside this confidence interval, a gain or loss in the tumour DNA is assumed according to published criteria [22, 37].

The DOP-PCR products of each microdissected tissue area were purified using push columns (BioRad, Munich, Germany) to separate remaining DOP-PCR primer. Oligonucleotide primers for three loci on chromosome 8p (D8S137, NEFL, LPL5GT) were used [32, 40]. Microsatellite PCRs were carried out in a 50-µl reaction volume with 0.5 µl [α^{33}P] dATP (1000–3000 Ci/mmol, Amersham Buchler, Braunschweig, Germany), 1.2 µl dNTPs (5 mM dATP, 10 mM dCTP, 10 mM dGTP, 10 mM dTTP), 0.2 mM primer, 1 µl DOP-PCR product and 4 units Taq polymerase. 'Hot start' PCR was performed, which consisted of 35 cycles (94°C for 1 min, 58°C/52°C for 30 s, 72°C for 2 min; final extension: 72°C for 7 min). Radioactively labelled PCR products were separated on a 6% polyacrylamide gel according to standard procedures. For visualization of labelled microsatellite repeats, Kodak Biomax MR scientific imaging film (Rochester, N.Y.) was exposed overnight and for 2 days.

Results

CGH data from the primary tumour were obtained from nine different samples containing various numbers of cells. These were frozen tissue without microdissection (approximately 10^7 cells) or formalin-fixed and paraffin-embedded tissue from which either high (approximately 10^5 cells) or low (50–100 cells) cell numbers were obtained by microdissection. In the frozen tissue, CGH revealed gains on chromosomes 7, 11q12→q13, 16p12→p13, 19, 20q22 and losses on chromosomes 12p11→p12 and 13q21→q34 (Table 1). The tumour sample containing approximately 10^5 cells microdissected from the paraffin sections showed a gain of DNA sequences only on 16p12→p13, and losses on chromosomes 2p25, 4q33→q35, 8p21→p23, 11q24→q25, 12p11→p12, 12q21→q26, 18q22, and Xq26→q28.

Four different areas of the primary tumour were randomly selected from a H&E-stained paraffin section, and 50 to 100 cells from each were removed after laser-assisted microdissection. These areas displayed different histological patterns: cribriform (area I), tubular (area II), solid (area III), or papillary (area IV). An example for microdissection of a small cell group from a tumour area exhibiting a cribriform pattern is demonstrated in Fig. 1 A–D. To obtain sufficient amounts of DNA for CGH, DOP-PCR amplification of genomic DNA was performed on

Table 1 CGH results from 9 different samples of a primary and metastatic prostatic adenocarcinoma and PINs

Chromosomal changes detected by CGH	Primary tumour (frozen tissue[a])	Primary tumour (Paraffin-embedded tissue[b])	Primary tumour (microdissected area I[c], cribriform)	Primary tumour (microdissected area II[c], tubular)	Primary tumour (microdissected area III[c], solid)	Primary tumour (microdissected area IV[c], papillary)	Low-grade PIN[3)]	High-grade PIN[3)]	Lymph node metastasis (paraffin-embedded tissue)[b]
Gains on chromosomes:									
1p32→p36	–	–	+	+	–	+	–	–	–
2p22	–	–	+	–	–	+	–	–	–
3q21	–	–	+	–	+	+	–	–	–
7	+	–	+	–	+	+	+	–	–
8q21→q24	–	–	+	+	+	–	+	+	–
11q12→q13	+	–	+	+	+	+	–	+	–
12q15→q21	–	–	–	–	–	–	+	–	–
16p12→p13	+	+	+	+	–	+	+	–	+
16q21→q23	–	–	–	+	–	–	–	–	–
17	–	–	–	+	+	+	+	+	–
19	+	–	–	+	+	+	–	–	+
20q22	+	–	–	–	–	+	–	+	–
Losses on chromosomes:									
2p25	–	+	–	–	–	–	+	–	+
3p25→p27	–	–	–	–	–	–	–	–	+
4q33→q35	–	+	–	–	–	–	–	–	+
8p21→p23	–	+	–	–	+	–	+	–	+
9p24	–	–	–	–	–	–	–	–	+
11q24→q25	–	+	–	–	–	–	–	–	+
12p11→p12	+	+	–	–	+	–	–	–	–
12q21→q26	–	+	–	–	+	–	–	+	–
13q21→q34	+	–	+	–	–	–	–	–	+
16q12	–	–	–	–	+	–	–	–	–
16q23	–	–	–	–	+	+	–	–	–
18q22	–	+	–	+	–	–	–	–	–
Xq26→q28	–	+	–	–	–	–	–	–	+

[a)] CGH results obtained from approx. 10^7 cells
[b)] CGH results obtained from approx. 10^5 cells
[c)] CGH results obtained from 50–100 cells

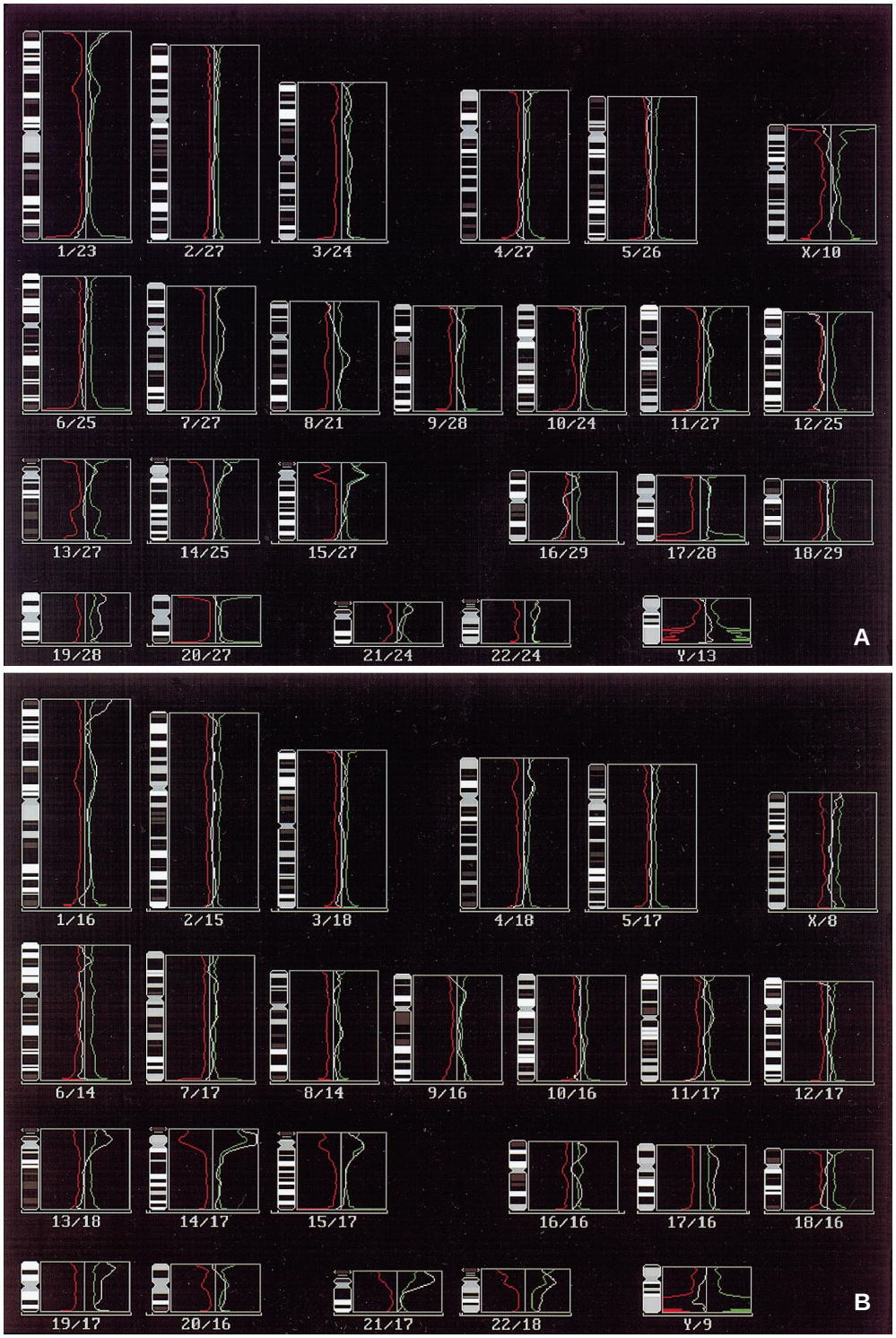

Fig. 2A, B Averaged profiles with statistical confidence limits are demonstrated for degenerate oligonucleotide (DOP)-PCR-generated DNA from microdissected tumour areas III, (solid **A**) and II (tubular **B**). For the tubular area, gains on 1p32→p36, 8q21→q24, 11q12→q13, 16p12→p13, 16q21→q23, 17, 19, and 22, and loss on 18q22 were diagnosed. The solid tumour area revealed gains on 3q, 7 8q21→q24, 11q12→q13, 17, 19, and 22, and losses on 4q33→q35, 8p21→p23, 12p, 12q, 16q12, and 16q23

samples containing 50 to 100 cells. CGH results of microdissected areas I–IV are summarized in Table 1, and they obviously indicate distinct intratumour heterogeneity. Recurrent chromosomal imbalances, repeatedly detected in at least two microdissected areas, were gains on chromosomes 1p32→p36, 2p22, 3q21, 7, 8q21→q24, 11q12→q13, 16p12→13, 17, 19 and loss on chromosome 16q23. Other chromosomal changes were found in only one of the microdissected tumour areas (Table 1). Gains on chromosome 16p12→p13 were found in higher cell numbers from paraffin-embedded and frozen tissue and in three microdissected tumour areas.

In addition, epithelial cells from PIN lesions that appeared outside the invasive tumour component were investigated after microdissection (Fig. 1E, F) and DOP-PCR amplification of genomic DNA. Gains of chromo-

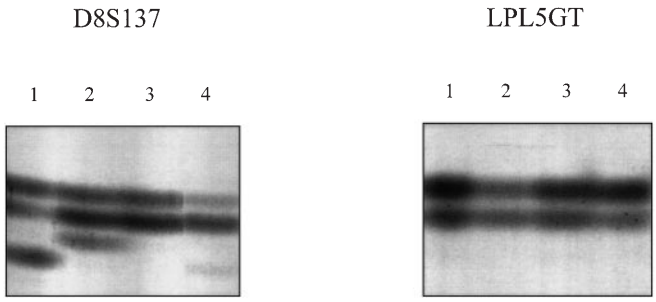

Fig. 3 Microsatellite analysis for 8p-loci D8S137 (*left*) and LPL5GT (*right*) performed on DOP-PCR products from microdissected areas of case P 64. DNA samples (from *left* to *right*): *1* invasive tumour area I, *2* normal epithelium, *3* invasive tumour area II, *4* high-grade PIN. D8S137: While invasive tumour area II showed allelic loss, the invasive tumor area I and the high-grade PIN exhibited allelic instability; LPL5GT: no allelic imbalances were detected for any of the microdissected tissue areas

somes 8q21→q24 and 17 were found in both low- and high-grade PINs. However, overrepresentation of DNA sequences on chromosomes 7, 11q, 12q, 16p, and 20q and underrepresentation of DNA sequences on chromosomes 2p, 8p and 12q were present in only one PIN lesion. With the exception of the observed loss on 12q15→q21, these abnormalities were also found in some of the investigated samples from the invasive tumour (Table 1). Approximately 80 microdissected cells obtained from normal prostatic epithelium outside the invasive tumour or PIN areas revealed no chromosomal imbalances by CGH after DOP-PCR. The lymph node metastasis (approximately 10^5 cells) showed chromosomal imbalances similar to those observed in higher cell numbers from the paraffin-embedded primary tumour (Table 1), but losses on 3p25→p27 and 9p24 were seen only in the metastatic tumour.

Figure 2 shows the averaged profiles with statistical confidence limits of two microdissected tumour areas (areas II and III). To validate selected CGH results, microsatellite analysis of chromosomal region 8p21→p22 was performed on DOP-PCR amplification products and genomic DNA isolated from high cell numbers of both the primary tumour and the lymph node metastasis. As shown in Fig. 3, DOP-PCR amplification products are suitable templates for a subsequent microsatellite analysis. The *LPL5GT* locus, which is located proximal to *D8S137* and *NEFL*, showed no allelic imbalance in any of the microdissected samples. However, both *D8S137* and *NEFL* exhibited either allelic loss or gain in some of the tumour and PIN samples (Table 2, Fig. 3).

Discussion

Methodological improvements of approaches combining microdissection and CGH analysis [24] were prerequisites for the characterization of early chromosomal changes in cervical carcinoma [15] and intraductal breast cancer [23]. However, the identification of such early events in premalignant lesions of prostatic carcinomas requires further modification of the microdissection/CGH approach, since PIN is present as very small cell groups on 5-µm sections, which means far fewer cells available than from cervical dysplasia or carcinoma in situ of the breast. Moreover, the investigation of cytogenetic aberrations of distinct histological patterns, or of the multiple foci that may be present in prostatic adenocarcinoma, depends upon a reliable CGH analysis of small cell groups.

Kuukasjärvi et al. [24] diluted DNA of a cell line (MCF-7) down to 50 pg and obtained reliable CGH results after DOP-PCR amplification of the template DNA. The estimated sensitivity of this experiment using diluted DNA corresponds to approximately two MCF-7 cells. In paraffin sections of surgical specimens of intraductal breast carcinoma, CGH was successfully performed from one to two microdissected ducts containing roughly 500–1000 cells [23, 24]. In order to analyse the smaller cell numbers of PIN lesions or invasive tumour cell groups with a distinctive histological pattern in prostatic adenocarcinoma, we optimized laser-assisted microdissection and CGH to characterize 50–100 cell compartments. With this approach, the four invasive tumour cell samples of the prostatic adenocarcinoma examined displayed chromosomal imbalances (gains on 2p, 3q, 7, 8q, 16p; losses on 8p, 9p, 13q, 16q, 18q; Table 1) that corresponded to gains and losses already described in these tumours [8, 20, 26, 34, 41].

Table 2 Microsatellite instability in eight samples of primary and metastatic adenocarcinoma and PINs (• Microsatellite instability detected, ∗ Microsatellite instability not detected)

Microsatellite locus	Primary tumour (Paraffin-embedded tissue[a])	Primary tumour (micro-dissected area I[b], cibriform)	Primary tumour (micro-dissected area II[b], tubular)	Primary tumour (micro-dissected area III[b], solid)	Primary tumour (micro-dissected area IV[b], papillary)	Low-grade PIN[b])	High-grade PIN[b])	Lymph node metastasis (paraffin-embedded tissuea)
D8S137 (8p21)	•	∗	•	•	•	•	•	•
NEFL (8p21)	•	∗	•	∗	•	•	∗	•
NPL (8p22)	∗	∗	∗	∗	∗	∗	∗	∗

[a)] CGH results obtained from approx. 10^5 cells
[b)] CGH results obtained from 50–100 cells

However, these chromosomal changes were not consistently detected in all four microdissected tumour areas. Gains on 16q and losses on 8p, previously reported as recurrent aberrations in prostate cancer [8, 41], were found only in one of the four samples. Thus, an intratumour heterogeneity became apparent at the cytogenetic level that was previously histologically evident in the four tumour areas analysed. These data are supported by earlier studies of prostatic adenocarcinomas demonstrating intratumour and intraglandular genetic heterogeneity by FISH and microsatellite analysis [18, 28, 30]. In contrast to FISH analysis, in which only known sequences are targeted, CGH allows the screening of the entire genome for unknown DNA copy number changes. Thus, CGH from microdissected cell groups can be used to assess cytogenetic changes in different histological patterns that are usually present in a prostatic cancer specimen, such as the different Gleason patterns.

Although Kuukasjärvi et al. [24] have demonstrated that CGH can be reliably performed from very small DNA amounts after DOP-PCR amplification, we have validated our data by additional studies. Microsatellite analyses and FISH results [2] were in accordance with our CGH results. Moreover, CGH without preceding DOP-PCR in tumour samples containing high cell numbers, that is to say 10^5 cells from paraffin sections or 10^7 cells from frozen tissue, confirmed most of the changes found in the four small microdissected areas. In the present study, artefacts of the combined microdissection/DOP-PCR/CGH approach can be excluded, since investigation of approximately 80 cells from normal prostatic glands outside the tumour revealed no chromosomal imbalances. This supports the accuracy of the method described. However, on the basis of our experience of using DOP-PCR for complete genomic DNA amplification, extreme care must be taken to avoid any contamination of PCR reagents with unknown DNA. Therefore, control experiments such as are described in the ”Materials and methods” section are indispensable whenever DOP-PCR amplification is performed. Methodological problems may occur in the interpretation of telomeric regions by CGH, especially if biotin- and digoxigenin-labelled DNA probes are used [11]. In our study some of the reported changes are located near telomeric regions, but they mostly cover more than a single chromosomal band. Moreover, telomeric regions did not reveal chromosomal imbalances in our control hybridizations (reference DNA against reference DNA or reference DNA against microdissected normal cells), for which biotin- and digoxigenin-labelled probes were also used. Thus, it seems unlikely that chromosomal imbalances near the telomeric regions have been misinterpreted.

This is the first study that has investigated PIN by CGH. Although only a single case has been investigated in this study, which does not allow a definitive conclusion on tumour progression in the prostate, we have demonstrated that a number of chromosome changes (gains on 7, 8q,11q, 16p, 17, 20q; losses on 8p, 12q) were present in the invasive tumour areas and even in low- and/or high-grade PIN in the surrounding tissue. Interestingly, results from recent FISH analyses have suggested that gains of chromosome 8 and c-*myc* (8q24) overexpression detected in PINs and lymph node metastases may represent markers of tumour progression [18]. Our data from two PIN lesions also exhibited a gain on 8q21→q24 and thus support the reported FISH results. Some chromosomal imbalances found in the lymph node metastasis (loss on 8p and 13q) have also been described by Cher et al. [8] as markers of metastatic potential in prostate cancer.

We conclude that a combined approach with laser-assisted microdissection, DOP-PCR and CGH is suitable for the identification of chromosomal imbalances associated with particular histological patterns of tumour tissue. Our CGH results further indicate that PIN is a likely precursor lesion for prostatic adenocarcinoma and that intratumour genetic heterogeneity is present among various primary tumour areas and metastases.

Acknowledgements The skilful technical assistence of S. Holthaus and S. Schulte Overberg is gratefully acknowledged. This work was supported in part by the Deutsche Forschungsgemeinschaft (DFG; contract Ho 1258/2-2).

References

1. Alers CA, Krijtenburg PJ, Vissers KJ, Bosman FT, van der Kwast TH, Dekken H (1995) Interphase cytogenetics of prostatic adenocarcinoma and precursor lesions: analysis of 25 radical prostatectomies and 17 adjacent prostatic intraepithelial neoplasias. Genes Chromosom Cancer 12:241–250
2. Aubele M, Zitzelsberger H, Szücs S, Werner M, Braselmann H, Hutzler P, Rodenacker K, Lehmann L, Minkus G, Höfler H (1997) Comparative FISH analysis of numerical chromosome 7 abnormalities in 5 µm and 15 µm paraffin-embedded tissue sections from prostatic carcinoma. Histochem Cell Biol 107: 121–126
3. Becker I, Becker KF, Röhrl MH, Minkus G, Schütze K, Höfler H (1996) Single-cell mutation analysis of tumors from stained histologic slides. Lab Invest 75:801–807
4. Bockmühl U, Schwendel A, Dietel M, Petersen I (1996) Distinct patterns of chromosomal alterations in high- and low-grade head and neck squamous cell carcinomas. Cancer Res 56:5325–5329
5. Bostwick DG, Montironi R (1997) Evaluating radical prostatectomy specimens: therapeutic and prognostic importance. Virchows Arch 430:1–16
6. Brothman AR, Watson MJ, Zhu XL, Williams BJ, Rohr LR (1994) Evaluation of 20 archival prostate tumor specimens by fluorescence in situ hybridization (FISH). Cancer Genet Cytogenet 75:40–44
7. Brown JA, Alcaraz A, Takahashi S, Persons DL, Lieber MM, Jenkins RB (1994) Chromosomal aneusomies detected by fluorescent in situ hybridization analysis in clinically localized prostate carcinoma. J Urol 152:1157–1162
8. Cher ML, Bova GS, Moore DH, Small EJ, Carroll PR, Pin SS, Epstein JI, Isaacs WB, Jensen RH (1996) Genetic alterations in untreated metatases and androgen-independent prostate cancer detected by comparative genomic hybridization and allelotyping. Cancer Res 56:3091–3102
9. Deubler DA, Williams BJ, Zhu XL, Steele MR, Rohr LR, Jensen JC, Stephenson RA, Changus JE, Miller GJ, Becich MJ, Brothman AR (1997) Allelic loss detected on chromosomes 8, 10, and 17 by fluorescence in situ hybridization using single-copy P1 probes on isolated nuclei from paraffin-embedded prostate tumors. Am J Pathol 150:841–850

10. Du Manoir S, Speicher MR, Joos S, Schröck E, Popp S, Dohner H, Kovacs G, Robert-Nicoud M, Lichter P, Cremer T (1993) Detection of complete and partial chromosome gains and losses by comparative genomic hybridisation. Hum Genet 90:590–610
11. Elrifai W, Larramendy ML, Bjorkqvist AM, Hemmer S, Knuutila S (1997) Optimization of comparative genomic hybridization using fluorochrome conjugated to dCTP and dUTP nucleotides. Lab Invest 77:699–700
12. Emmert-Buck MR, Bonner RF, Smith PD, Chuaqui RF, Zhuang Z, Goldstein SR, Weiss RA, Liotta LA (1996) Laser capture microdissection. Science 274:998–1001
13. Greulich KO, Leitz G (1994) Light as microsensor and micromanipulator: laser microbeams and optical tweezers. Exp Techn Phys 40:1–14
14. Guan XY, Trent JM, Meltzer PS (1993) Generation of band-specific painting probes from a single microdissected chromosome. Hum Mol Genet 2:1117–1121
15. Heselmeyer K, Schröck E, du Manoir S, Blegen H, Shah K, Steinbeck R, Auer G, Ried T (1996) Gain of chromosome 3q defines the transition from severe dysplasia to invasive carcinoma of the uterine cervix. Proc Natl Acad Sci USA 93:479–484
16. Huang S-F, Xiao S, Renshaw AA, Loughlin KR, Hudson TJ, Fletcher JA (1996) Fluorescence in situ hybridization evaluation of chromosome deletion patterns in prostate cancer. Am J Pathol 149:1565–1573
17. Isola J, DeVries S, Chu L, Ghazvini S, Waldman F (1994) Analysis of changes in DNA sequence copy number by comparative genomic hybridisation in archival paraffin-embedded tumour samples. Am J Pathol 145:1301–1308
18. Jenkins RB, Qian J, Lieber MM, Bostwick DG (1997) Detection of c-myc oncogene amplification and chromosomal anomalies in metastatic prostatic carcinoma by fluorescence in situ hybridization. Cancer Res 57:524–531
19. Johnson GD, de Nogueira Araujo GM (1981) A simple method of reducing the fading of immunofluorescence during microscopy. J Immunol Methods 43:349–350
20. Joos S, Bergerheim US, Pan Y, Matsuyama H, Bentz M, du Manoir S, Lichter P (1995) Mapping of chromosomal gains and losses in prostate cancer by comparative genomic hybridisation. Genes Chromosom Cancer 14:267–276
21. Kallioniemi A, Kallioniemi OP, Sudar D, Rutovitz D, Gray JW, Waldman F, Pinkel D (1992) Comparative genomic hybridization for molecular cytogenetic analysis of solid tumors. Science 258:818–821
22. Kallioniemi OP, Kallioniemi A, Piper J, Isola J, Waldman FM, Gray JW, Pinkel D (1994) Optimizing comparative genomic hybridization for analysis of DNA sequence copy number changes in solid tumors. Genes Chromosom Cancer 10:231–243
23. Kuukasjärvi T, Tanner M, Pennanen S, Karhu R, Kallioniemi O-P, Isola J (1997) Genetic changes in intraductal breast cancer detected by comparative genomic hybridization. Am J Pathol 150:1465–1471
24. Kuukasjärvi T, Tanner M, Pennanen S, Karhu R, Visakorpi T, Isola J (1997) Optimizing DOP-PCR for universal amplification of small DNA samples in comparative genomic hybridization. Genes Chromosom Cancer 18:94–101
25. Lehmann L, Greulich K, Zitzelsberger H, Negele T, Spelsberg F, Bauchinger M, Weier HU (1997) Cytogenetic and molecular genetic characterization of a chromosome 2 rearrangement in a case of human papillary thyroid carcinoma with radiation history. Cancer Genet Cytogenet 96:30–36
26. Li C, Larsson C, Futreal A, Lancaster J, Phelan C, Aspenblad U, Sundelin B, Liu Y, Ekman P, Auer G, Bergerheim USR (1998) Identification of two distinct deleted regions on chromosome 13 in prostate cancer. Oncogene 16:481–487
27. Macoska JA, Trybus TM, Sakr WA, Wolf MC, Benson PD, Powell IJ, Pontes JE (1994) Fluorescence in situ hybridization analysis of 8p allelic loss and chromosome 8 instability in human prostate cancer. Cancer Res 54:3824–3830
28. Macintosh CA, Stower M, Reiid N, Maitland NJ (1998) Precise microdissection of human prostate cancers reveals genotypic heterogeneity. Cancer Res 58:23–28
29. Matsuyama H, Pan Y, Skoog L, Tribukait B, Naito K, Ekman P, Lichter P, Bergerheim US (1994) Deletion mapping of chromosome 8p in prostate cancer by fluorescence in situ hybridization. Oncogene 9:3071–3076
30. Qian J, Bostwick DG, Takahashi S, Borell TJ, Brown JA, Lieber MM, Jenkins RB (1996) Comparison of fluorescence in situ hybridization analysis of isolated nuclei and routine histological sections from paraffin-embedded prostatic adenocarcinoma specimens. Am J Pathol 149:1193–1199
31. Ried T, Knutzen R, Steinbeck R, Blegen H, Schröck E, Heselmeyer K, du Manoir S, Auer G (1996) Comparative genomic hybridisation reveals a specific pattern of chromosomal gains and losses during the genesis of colorectal tumours. Genes Chromosom Cancer 15:234–245
32. Rogaev E, Rogaeva E, Lukiw WJ, Vaula G, Liang Y, Hancock R, McLachlan DC, George-Hyslop PHSt (1992) An informative microsatellite repeat polymorphism in the human neurofilament light polypeptide (NEFL) gene. Hum Mol Genet 1: 781
33. Ruijter ET, van de Kaa CA, Schalken JA, Debruyne FM, Ruiter DJ (1996) Histological grade heterogeneity in multifocal prostate cancer. Biological and clinical implications. J Pathol (Lond) 180:295–299
34. Sauter G, Bubendorf L, Moch M, Gasser TC, Mihatsch MJ (1998) Cytogenetic alterations in prostate cancer. Pathologe 19:63–68
35. Schütze K, Clement-Sengewald A (1994) Catch and move – cut or fuse. Nature 368:667–669
36. Sobin LH, Wittekind C (ed) (1997) TNM classification of malignant tumours. Wiley-Liss, New York
37. Solinas-Toldo S, Wallrapp C, Müller-Pillasch F, Bentz M, Gress T, Lichter P (1996) Mapping of chromosomal imbalances in pancreatic carcinoma by comparative genomic hybridisation. Cancer Res 56:3803–3807
38. Speicher MR, du Manoir S, Schröck E, Holtgreve-Grez H, Schoell B, Lengauer C, Cremer T, Ried T (1993) Molecular cytogenetic analysis of formalin-fixed, paraffin-embedded solid tumors by comparative genomic hybridization after universal DNA-amplification. Hum Mol Genet 2:1907–1914
39. Telenius H, Carter NP, Bebb ChE, Nordenskjöld M, Ponder BAJ, Tunnacliffe A (1992) Degenerate oligonucleotide-primed PCR: general amplification of target DNA by a single degenerate primer. Genomics 13:718–725
40. Tomfohrde J, Wood S, Schertzer M, Wagner MJ, Wells DE, Parrish J, Sadler LA, Blanton SH, Daiger SP, Wang Z, Wilkie PJ, Weber JL (1992) Human chromosome 8 linkage map based on short tandem repeat polymorphisms: effect of genotyping errors. Genomics 14:144–152
41. Visakorpi T, Kallioniemi AH, Syvänen AC, Hyytinen ER, Karhu R, Tammela T, Isola JJ, Kallioniemi OP (1995) Genetic changes in primary and recurrent prostate cancer by comparative genomic hybridization. Cancer Res 55:342–347
42. Wiltshire RN, Duray P, Bittner ML, Visakorpi T, Meltzer PS, Tuthill RJ, Liotta LA, Trent JM (1995) Direct visualisation of the clonal progression of primary cutaneous melanoma: application of tissue microdissection and comparative genomic hybridisation. Cancer Res 55:3954–3957
43. Zhuang Z, Bertheau P, Emmert-Buck MR, Liotta LA, Gnarra J, Linehan WM, Lubensky IA (1995) A microdissection technique for archival DNA analysis of specific cell populations in lesions <1 mm in size. Am J Pathol 146:620–625
44. Zitzelsberger H, Szücs S, Weier H-U, Lehmann L, Braselmann H, Enders S, Schilling A, Breul J, Höfler H, Bauchinger M (1994) Numerical abnormalities of chromosome 7 in human prostate cancer detected by fluorescence in situ hybridization (FISH) on paraffin-embedded tissue section with centromere-specific DNA probes. J Pathol (Lond) 172:325–335